JOURNAL OF AGRICULTURAL AND FOOD CHEMISTRY

HlMyb3, a Putative Regulatory Factor in Hop (*Humulus lupulus* L.), Shows Diverse Biological Effects in Heterologous Transgenotes

JAROSLAV MATOUŠEK,[†‡] TOMÁŠ KOCÁBEK,[†] JOSEF PATZAK,[§] JOSEF ŠKOPEK,[†] LINA MALOUKH,[∥] ARNE HEYERICK,[⊥] ZOLTÁN FUSSY,[‡] ISABEL ROLDÁN-RUIZ,[∥] AND DENIS DE KEUKELEIRE*[,⊥]

Biology Centre of the ASCR, v.v.i. Institute of Plant Molecular Biology, Branišovská 31, 370 05 České Budějovice, Czech Republic, Faculty of Biological Sciences, University of South Bohemia, Branišovsk 31, 37005, Česke Budějovice, Czech Republic, Hop Research Institute GmbH, Kadaňská 2525, 438 46 Žatec, Czech Republic, Department of Plant Genetics and Breeding, Agricultural Research Centre, Caritasstraat 21, B-9090 Melle, Belgium, and Laboratory of Pharmacognosy and Phytochemistry, Faculty of Pharmaceutical Sciences, Ghent University, Harelbekestraat 72, B-9000 Ghent, Belgium

A hop-specific cDNA library from glandular tissue-enriched hop cones was screened for Myb transcription factors. cDNA encoding for R2R3 Myb, designated *HlMyb3*, was cloned and characterized. According to the amino acid (aa) sequence, *HlMyb3* shows the highest homology to *GhMyb5* from cotton and is unrelated to the previously characterized *HlMyb1* from the hop. Southern blot analyses indicated that *HlMyb3* is a unique gene, which was detected in various *Humulus lupulus* cultivars, but not in *Humulus japonicus*. Reverse transcription and real-time PCR revealed the highest levels of *HlMyb3* mRNA in hop cones at a late stage of maturation and in colored petiole epidermis, while the lowest levels were observed in hop flowers. Two alternative open reading frames starting in the *N*-terminal domain of *HlMyb3*, encoding for proteins having 269 and 265 amino acids with apparent molecular masses of 30.3 and 29.9 kDa, respectively, were analyzed as transgenes that were overexpressed in *Arabidopsis thaliana*, *Nicotiana benthamiana*, and *Petunia hybrida* plants. Transformation with the longer 269 aa variant designated *l-HlMyb3* led to a flowering delay and to a strong inhibition of seed germination in *A. thaliana*. Nearly complete flower sterility, dwarfing, and leaf curling of *P. hybrida* and *N. benthamiana l-HlMyb3* transgenotes were noted. On the contrary, the shorter 265-aa-encoding *s-HlMyb3* transgene led in *A. thaliana* to the stimulation of initial seed germination, to fast initiation of the lateral roots, and to quite specific branching phenotypes with many long lateral stems formed at angles near 90°. Limited plant sterility but growth stimulation and rather branched phenotypes were evident for *s-HlMyb3* transgenotes of *P. hybrida* and *N. benthamiana*. It was found that both *HlMyb3* transgenes interfere in the accumulation and composition of flavonol glycosides and phenolic acids in transformed plants. These effects on heterologous transgenotes suggest that the *HlMyb3* gene may influence hop morphogenesis, as well as metabolome composition during lupulin gland maturation.

KEYWORDS: Plant transcriptional factors; hop cDNA library; *Arabidopsis thaliana*; *Nicotiana benthamiana*; *Petunia hybrida*; secondary metabolites; plant morphogenesis; plant transformation

INTRODUCTION

Hop (*Humulus lupulus* L.) is a dioecious perennial climbing plant cultivated for commercial use in the brewing industry and has been known in traditional medicine since medieval times. Hop female inflorescences, referred to as cones, contain glandular trichomes (lupulin glands) that form a specific part of the hop metabolome characterized by a relatively stable biochemical composition that is typical for each individual hop genotype (*1*). In addition to the main constituents known as humulones or α-acids and lupulones or *β*-acids that are valuable flavor-active ingredients for beer brewing, several compounds in the lupulin metabolome including prenylated flavonoids have recently aroused high interest in view of their potent medicinal activities (*2*). Xanthohumol (X; up to 1.3%, m/m, of the dry

* Author to whom correspondence should be addressed. Tel.: +32-9-264-8055. Fax: +32-9-264-8192. E-mail: Denis.DeKeukeleire@UGent.be.
[†] v.v.i. Institute of Plant Molecular Biology.
[‡] University of South Bohemia.
[§] Hop Research Institute.
[∥] Agricultural Research Centre.
[⊥] Ghent University.

10.1021/jf071153+ CCC: $37.00
Published on Web 08/21/2007

weight of a hop cone) and desmethylxanthohumol (DMX; up to 0.2%) are the principal prenylated chalcones in the lupulin glands. These chalcones are prone to undergo an intramolecular Michael-type cycloaddition leading to prenylated flavanones. Thus, X gives rise to isoxanthohumol (IX, the predominant prenylated flavonoid in beer), and DMX leads to a mixture of 8-prenylnaringenin (8-PN) and 6-prenylnaringenin (6-PN). X is a fascinating cancer-chemopreventive compound exhibiting a broad spectrum of inhibition mechanisms at all stages of carcinogenesis (*3*), while 8-PN is one of the most potent phytoestrogens currently known (*4*).

The total yield of valuable compounds in hops not only depends on the content and the composition of the lupulin metabolome, that continuously vary during cone maturation, but also on another genetic component determining the number and size of hop cones and the density of the trichomes. The maximal number of cones on a hop plant depends on the bine internode length, the total height, and the formation of lateral branches and their length and density, as well as on the number of cones on laterals. Hence, the total cone yield relates to the overall morphology of the plant.

Recent analyses discovered several structural genes encoding for chalcone synthase (EC 2.3.1.74; CHS) (*5*) or CHS-like enzymes (e.g. ref *6*) that are likely to be involved in the biosynthesis of the lupulin metabolome. Especially, the chalcone synthase CHS_H1 (*5*) forming an oligofamily of identical members relative to the catalytical core (*7*) has been shown to be able to catalyze the formation of both chalcones as precursors of X, as well as humulones and lupulones (*8*). Other studies (*7, 9*) document that the number of structural *chs* genes cannot simply explain differences among various cultivars, suggesting that the genotype-specific diversity is rather mediated by a combinatorial action of regulatory genes. The sequence analysis of the *chs*_H1 promoter region revealed specific Myb-binding motifs (*7, 9*), and accordingly, *chs*_H1 activation in response to the R2R3 PAP1 Myb factor from *A. thaliana* was found (*7*). This indicates that Myb homologs are involved in *chs*_H1 regulation in the hop.

In addition to the involvement of Myb transcription factors (TFs) in the regulation of the flavonoid biosynthetic pathways (e.g., ref *10*), *R2R3* Myb factors specifically regulate a number of other plant-specific processes (*11*). For instance, it is known that Myb's play very important roles regarding cell fate (e.g., ref *12*), meristem and vascular system differentiation (e.g., ref *13*), apical dominancy, axillary bud signaling and branching (*14–16*), and trichome and epidermis differentiation (*17, 18*). It is of great interest to analyze hop Myb homologs involved in apical dominance and branching regulation, as well as in glandular trichome differentiation and maturation.

It is obvious from recent studies that some Myb TFs interact with other TFs and form more complicated complexes like the Myb–bHLH–WD40 complex that mediates the diversification of cell differentiation pathways (*12*) or the activation of biochemical pathways like anthocyanin production (*19*). Probably due to combinatorial interaction (*20*), certain Myb regulators enter complicated networks and exhibit pleiotropic or secondary effects that are observed also in heterologous transgenotes (e.g., refs *21* and *22*).

In our previous work, we isolated and characterized the first Myb-like TF from *H. lupulus* using a cDNA library from glandular tissue-enriched hop flowers and maturating cones (*9*). This TF is clustering together with a group of R2R3 P-like Mybs (*23*) from *Zea mays* controlling flavonoid biosynthesis and the Blind factor from the tomato (*15*). In the present study, we characterized a new putative regulatory element isolated from hop cones via cDNA library screening. Although this unique TF, designated *HlMyb3*, is highly expressed in maturating hop cones and in the colored epidermis tissue of hop petioles, it is unrelated to the previously published TF, *HlMyb1*. Rather than relying on direct laborious and time-consuming hop transformations (*24*), we used a much more efficient *Agrobacterium tumefaciens*-mediated transformation of *Arabidopsis thaliana*, *Nicotiana benthamiana*, and *Petunia hybrida* (heterologous transgenotes) to assay possible effects of *HlMyb3* in plant transgenotes. Diverse morphological and physiological changes including shifts in metabolomes caused by subvariants of *HlMyb3* are reported.

MATERIALS AND METHODS

Plant Cultivation Conditions and Sampling. Czech fine aromatic red-bine hop (*Humulus lupulus* L.), Osvald's clone 72, other hop varieties as specified in the figure legends, and *H. japonicus* were grown under natural field conditions. For the analysis of RNA, samples were collected from the semiearly variety Osvald's clone 72 at several stages including flowers with green pistils; early stage, with cones up to 0.6 cm in length developing bracts and dried pistils; intermediate stage, with cones about 1 cm in length having green bracts; later stage, with cones of 1–1.5 cm in length and green bracts; and late stage, with cones exceeding 1.8 cm in length often showing traces of anthocyanin pigments on bract spikes. RNA was collected also from early, intermediate, and later stages of the middle- to early-flowering varieties Hallertau and Fuggle, as well as from the late-flowering varieties Agnus and Taurus during the period from June to the beginning of September in 2005 and 2006. Osvald's clone 72, *Petunia hybrida* cv. Andrea, and *Nicotiana benthamiana* plants were maintained in glass boxes at a temperature of 25 ± 3 °C. Plants were grown under natural light from March to July with supplementary illumination (170 μmol m^{-2} s^{-1} PAR) to maintain a 16-h-day period. *Arabidopsis thaliana* plants were grown in soil mixed with vermiculite (3:1) in the greenhouse or in the culture room. *A. thaliana* plants were maintained at the vegetative stage under an 8-h light photoperiod to get sufficient seed production. After the appearance of the first flower stems, the photoperiod was changed to 16 h of light. For the cultivation under in vitro conditions, the *A. thaliana*, *N. benthamiana*, and *P. hybrida* seeds were surface-sterilized with commercial bleach SAVO (Bochemie, Bohumín, Czech Republic) containing 1.6% sodium hypochlorite for 15 min, then rinsed (three times) with sterile distilled water, and finally plated on Petri dishes with a complete MS medium (Duchefa Biochemie, Haarlem, The Netherlands) containing 0.8% agar. The plants were cold-acclimated at 5 °C for 2 days to synchronize germination. The growing conditions for in vitro cultures were 22 ± 3 °C, an 8 h light/16 h dark photoperiod, and 150 μmol m^{-2} s^{-1} PAR light intensity. *P. hybrida* plants were cultivated in vitro on the MS medium containing 1.0% agar under conditions described by Matoušek et al. (*7*).

In some experiments, growth and development of *A. thaliana* transgenotes were compared in vitro. The seeds were surface-sterilized as described above and sowed on plastic square Petri dishes (120 × 120 mm) with a 1% agar MS medium. To synchronize germination, the plates with the seeds were kept for 3 days at 4 °C. The seeds were arranged in five rows. Each row contained approximately 20 seeds, which represented one line including the wild-type control ecotype Columbia. The dishes were kept in a vertical position at an angle near 75° in the culture cabinet (under conditions described above for in vitro cultures) for 3 weeks.

Analysis of Secondary Metabolites. Seedlings of *A. thaliana* and leaves of *N. benthamiana* and *P. hybrida* were lyophilized prior to the analysis of secondary metabolites. After grounding up lyophilized plant material in a mortar, samples of 10–20 mg were extracted in eppendorf tubes using 1 mL of methanol/water (1/1, v/v), and after sonication, the extraction mixtures were kept for 12 h at 4 °C. All extractions were carried out in triplicate. After centrifugation at 18000 rpm for 10 min, the supernatant was analyzed by high-performance liquid chromatography (HPLC) using a Waters 2690 Alliance Separations Module

and a Waters 996 Photodiode Array, operated by Millennium software (version 3.20) (Waters, Zellik, Belgium). The column was a Varian Omnispher C18 (250 × 4.6 mm, 5 μm) maintained at 35 °C, while the injection volume was 50 μL. Gradient elution over 60 min was applied from 15% of solvent B (methanol/acetonitrile, 1/1, v/v, with 0.025% formic acid) in solvent A (water with 0.025% formic acid) to 95% of solvent B in A. A high-performance liquid chromatography–mass spectroscopy (HPLC–MS) analysis was carried out using an Agilent Technologies 1200 Series coupled to an MSD SL detector, operated by an Agilent G1978A Multimode Ion Source (Agilent Technologies, Santa Clara, CA). The column was a Zorbax SB-C18 (3 mm × 150 mm, 3.5 μm) maintained at 35 °C, while the injection volume was 10 μL. Gradient elution over 60 min was applied from 15% of solvent C (methanol with 0.025% formic acid) in solvent A (water with 0.025% formic acid) to 95% of solvent C in A. Chromatograms at 320 and 350 nm were extracted from the 3D data, and peaks were characterized on the basis of their UV spectra and retention times. Peak integrations were carried out using standard parameters, and normalized peak areas were calculated by dividing peak areas by the sample weight and the area of the corresponding peak in the reference sample.

***HlMyb3* Cloning, Preparation of Plant Expression Vectors, and Transformations Procedures.** Initial primers derived from conserved domains of PAP1 (AC:AF325123) for detecting R2R3 *Myb*-specific sequences from hop, designated CPAP5′ and CPAP3′, were described previously (*18*). These primers were used for reverse transcription–polymerase chain reaction (RT–PCR) to amplify a short *Myb*-specific 75 base-pair (bp) cDNA fragment using RNA from hop cones as a template. From an internal part of this fragment, 5′HMyb (5′TTAAACTACTTGCGTCCAAG) and 3′HMyb (5′ATGAAGTTCAAGAATAAGAAGCTGTG3′) primers were derived and used for the PCR screening of a hop-specific cDNA library from glandular tissue-enriched hop cones as a source of a PCR template (*9*). A combination of the 5′HMyb primer with the M13 forward primer led to amplificaton of the 3′ portion of *Myb* cDNA, while, by combining 3′HMyb with the reverse primer, the 5′ part of the *Myb* cDNA was amplified from the hop cDNA library. Finally, 5′-start (5′CAAAAATGGATGGTCCCATG 3′) and 3′-end (5′ CATGGAATCTCAAATGCGTC 3′) primers were designed to amplify the complete *Myb* cDNA. Reamplifications of cDNA fragments (if necessary) were performed using high-fidelity *Pwo* polymerase (Roche Molecular Biochemicals, Basel, Switzerland). cDNA fragments were cloned in the pCR-Script SK(+) vector (Stratagene, La Jolla, CA), and automatic sequencing was performed as described previously (*9*).

For the preparation of plant expression vectors, two open reading frame (ORF) variants were amplified from the *HlMyb3* clone No 1700 (AC:AM501509). When the primer combinations 5′s-HopMyb3Apa (5′cgGGGCCCATGGGAGATCAATTATAT3′) × 3′HopMyb3Xba (5′cgTCTAGAATCTCAAATGCGTCACG3′) and 5′l-HopMyb3Apa (5′cgGGGCCCATGGATGGTCCCATGG3′) × 3′HopMyb3Xba (additive nucleotides are designated by small letters and restriction sites are underlined) were used, the *s-HlMyb3*and *l-HlMyb3* fragments were prepared, respectively. Amplified DNA fragments were treated with *Apa*I and *Xba*I restriction enzymes and ligated into the derivative of vector pRT-100 (*25*), designated pLV-68. From this intermediate vector, *35S:s-HlMyb3* and *35S:l-HlMyb3* expression cassettes were excised using *Asc*I and *Pac*I restriction enzymes and ligated in the *Asc*I- and *Pac*I-digested plant expression vector pLV-62 constructed previously (*7*). The resulting expression vectors pLV-71 and pLV-72 containing *s-HlMyb3* and *l-HlMyb3* sequences, respectively, were introduced by the freeze–thaw method into *A. tumefaciens* LBA 4404 for transformation of *A. thaliana* and *N. benthamiana*. *P. hybrida* has been transformed independently using the same vectors introduced into a vigorous EHA 101 *A. tumefaciens* strain (also suitable for hop transformation) (*24*).

P. hybrida and *N. benthamiana* plants were transformed according to the standard leaf disc method as described previously (*7*). Regenerated transformed plants were maintained on the medium containing 100 mg/L kanamycin and 200 mg/L timentin. *A. thaliana* ecotype Columbia plants were transformed by the floral dip method (*26*). Transformed seeds were selected on agar plates containing 50 mg/L kanamycin. Two-week-old kanamycin-resistant plants were transferred to the soil.

RNA Isolation, Reverse Transcription-Polymerase Chain Reaction (RT–PCR), Real-Time PCR, and Northern Blot Analyses. For RT–PCR and real-time PCR, total RNA was isolated from 100 mg of plant leaf tissue using CONCERT (Plant RNA Purification Reagent, Invitrogen, Carlsbad, CA) following RNA purification and DNA cleavage on columns (RNeasy Plant Total RNA kit, Qiagen, Hilden, Germany). One-step RT–PCR was performed using a Titan One Tube RT-PCR system including a high-fidelity *Pwo* polymerase (Roche Molecular Biochemicals, Basel, Switzerland). If not stated otherwise, reverse transcription was run for 30 min at 48 °C, and after denaturation at 94 °C over 2 min, PCR was started with cycles of 30 s at 94 °C, 30 s at 55 °C, and 60 s at 68 °C.

Real-time PCR quantification of *HlMyb3* mRNA was performed using primers C5′M3PCR (5′GACGTCAACAGCAAGCAATTC 3′) and C3′M3RT (3′GGCCTCTGA CGTGTCTGATG 3′). This PCR reaction led to amplification of the 201 bp product. The 7SL RNA product was used as a constitutive control. Approximately 301 bp 7SL cDNA was amplified using primers α (5′ TGTAACCCAAGTGGGGG 3′) and anti-*β* (5′GCACCGGCCCGTTATCC 3′) covering conserved motifs of hop 7SL RNA genes (*27*).

For the first strand cDNA synthesis, we used 2 μg of total RNA, 1 μg of oligo dT 25 biopolymer in the case of *HlMyb3* mRNA, and anti-*β* primer in the case of 7SL RNA, 5x first strand buffer, DTT (0.1 M), dNTP's (20mM), superase inhibitor (40U), and Superscript II Reverse Transcriptase (200U; Invitrogene). After 2 hours of incubation at 42 °C, the real-time PCR mixtures were prepared. This mix contained 8.5 μL of deionizated water, 12.5 μL of SYBR green, 0.75 μL of PCR primers (10 mM), and 2.5 μL of the template in a total volume of 25 μL. This mix (25 μL) was put onto a multiple-sample PCR well-plate, and reactions were performed in an ABI PRISM 7000 Sequence Detection System (Applied Biosystems, Foster City, CA). The following LightCycler experimental run protocol was used: 2 min at 50 °C for activating UNG (Uracil-DNA glycosylase), 1 cycle at 95 °C for 10 min for polymerase activation, and 45 cycles at 95 °C for 15 sec and 60 °C for 1 min, a melting curve program (60–95 °C with a heating rate of 0.1 °C per second and a continous fluorescence measurement), and finally a cooling step to 40 °C. The "Fit Point Method" was performed using the ABI 7000 software (Applied Biosystems, Foster City, CA) for measuring CP at a constant fluorescence level. Dilutions of *HlMyb3* clone No 1700 were prepared and used as a standard template for quantitative calculations.

For the Northern blot analysis, total RNA samples extracted using the CONCERT reagent were dissolved in DEPC-treated water. Aliquots of 35 μg each were separated on formaldehyde-denaturing agarose gel. After blotting onto Biodyne A transfer membranes (*Pall*, Hampshire, England), samples were hybridized to a full-length *HlMyb3* cDNA probe labelled with [α-^{32}P]dCTP having a specific activity of 1×10^7 cpm μg^{-1} of DNA mL^{-1}. Prehybridization and hybridization were carried out in a 50% formamide-based (pre-)hybridization buffer (*28*) at 50 °C. The final washing was performed in 0.5 × SSC plus 0.1 SDS at 55 °C for 20 min.

Isolation of DNA and Genomic Blots. Isolation of genomic DNA from the hop, *H. japonicus*, and from *A. thaliana*, *N. benthamiana*, and *P. hybrida* transgenic plants was performed according to Rogers and Bendich (*29*) from about 100 mg of frozen plant material. Genomic DNA (5 μg) from each plant was separately digested with 50 units of *Eco*RI in 100 μL reaction mixes that were incubated overnight at 37 °C. Digested DNA was subjected to ethanol/sodium acetate precipitation; dissolved in 25 μL of H_2O; and subjected to electrophoresis (16 h at 25 V in a 0.7% agarose gel), depurination (15 min in 0.25 M HCl), denaturation (30 min in 1.5 M NaCl, 0.5 M NaOH), and neutralization (20 min in 0.5 M Tris–HCl pH 7, 1.5 M NaCl), before being transferred using a capillary blot overnight with 20 × SSC to 0.45 μm of nylon positively charged membranes (Sigma). The membranes were then crosslinked [15 s at 70000 $\mu J/cm^2$ and oven-dried (20 min at 80 °C)]. Prehybridization (2 h at 65 °C in 30 mL) and hybridization (overnight at 65 °C in 20 mL) were carried out in a buffer according to Church and Gilbert (*30*) using a hybridization oven. The membranes were hybridized to a *HlMyb3* cDNA probe having a specific activity of 5×10^7 cpm/μg of DNA. PCR products were blotted using alkaline blots.

Other Methods. For Southern and Northern blot analyses, full-length *HlMyb3* cDNA probes were labelled with [α-^{32}P]dCTP using the Redivue [α-^{32}P] dCTP 3000 Ci mmol^{-1} Rediprime II random prime labeling system (Amersham Pharmacia Biotech, Freiburg, Germany). The autoradiograms were scanned using the TYPHOON PhosphoImager (Amersham Biosciences, Sunnyvale, CA) device, and the intensities of bands on the Northern blots were quantified using ImageQuant software (Molecular Dynamics, Sunnyvale, CA).

For the analysis of *A. thaliana* seedlings' growth intensity, individual samples were photographed and then measured and statistically treated with the "measure of the length and area" options using the LUCIA v.5.0 software (Laboratory Imaging, Prague, Czech Republic).

For phylogenetic comparisons of MybTF's, sequences from the GeneBank database were used, as indicated on the individual figures. Sequence analyses were carried out with DNASIS for Windows, version 2.5 (Hitachi Software Engineering Company, Ltd., Tokyo, Japan). The phylogenetic trees were generated using the neighbor-joining method in the ClustalW option of the DNASIS MAX software (Hitachi, MiralBio, South San Francisco, CA).

RESULTS

Cloning, Sequential, and Genomic Analyses of the Transcription Factor *HlMyb3* in Hop. In analogy to our previous work (*9*), the initial primers for detecting Myb-specific sequences in the hop were derived from the *A. thaliana* R2R3*Myb* gene PAP1 (AC:AF325123), which is known to be involved in the regulation of the phenylpropanoid biosynthetic pathway (*31*). The primers used for this amplification were designated cPAP5′ and cPAP3′ and covered conserved amino acid (aa) motifs KSCRLRWL and GNRWSLIA. The RT–PCR amplification using RNA from hop cones as a template resulted in a short 75-bp cDNA fragment exhibiting homology with other plant Myb TFs. From the internal part of this fragment (not shown), HMyb primers were derived (see Materials and Methods) and used for the screening of a hop-specific cDNA library from glandular tissue-enriched hop cones as a source of the PCR template (*9*). A combination of the 5′H-Myb primer with the M13 forward primer led to amplificaton of the 3′ portion of *Myb* cDNA, while by combining 3′H-Myb with the reverse primer, the 5′ part of the *Myb* cDNA was amplified from the hop cDNA library. Finally, 5′-start and 3′-end primers were designed (see Materials and Methods) to amplify the complete *Myb* cDNA.

The sequenced cDNA deposited into EMBL under AC: AM501509 encoded for a typical *R2R3Myb* protein, designated *HlMyb3*, having 269 aa's with an apparent molecular weight of 30.3 kDa and pI 6.19. Homology searching using WU-Blast2 showed the highest homology on amino acid level with the *Myb5* factor from *Gossypium hirsutum* (*GhMyb5*) having AC number of AF377316 (**Figure 1A**). The overall homology between *HlMyb3* and *GhMyb5* reached 72%. This homology was much higher within the R2R3 DNA-binding domain (DBD), reaching 91% at 82% amino acid identity. On the basis of the amino acid structure analysis performed for *GhMyb5* by Loguercio et al. (*32*), it was possible to identify the *N*-terminal domain via homology comparisons. Furthermore, two transregulatory regions (TRRs), a 40 amino acid basic region (TRR1) on the one hand and an acidic region (TRR2) within the *C*-terminal domain on the other hand, were also identified (**Figure 1A**).

The pI values of the *N*-terminal segment, TRR1, and TRR2 were calculated to be 4.03, 10.11, and 3.29, respectively. Within the *N*-terminal segment, an alternative start codon was observed (**Figure 1A**). A deduced protein encoded by a shorter ORF would have 265 amino acids and an apparent molecular weight of 29.9 kDa. It was calculated that the pI of the *N*-terminal domain of the shorter *HlMyb3* (*s-HlMyb3*) variant would be

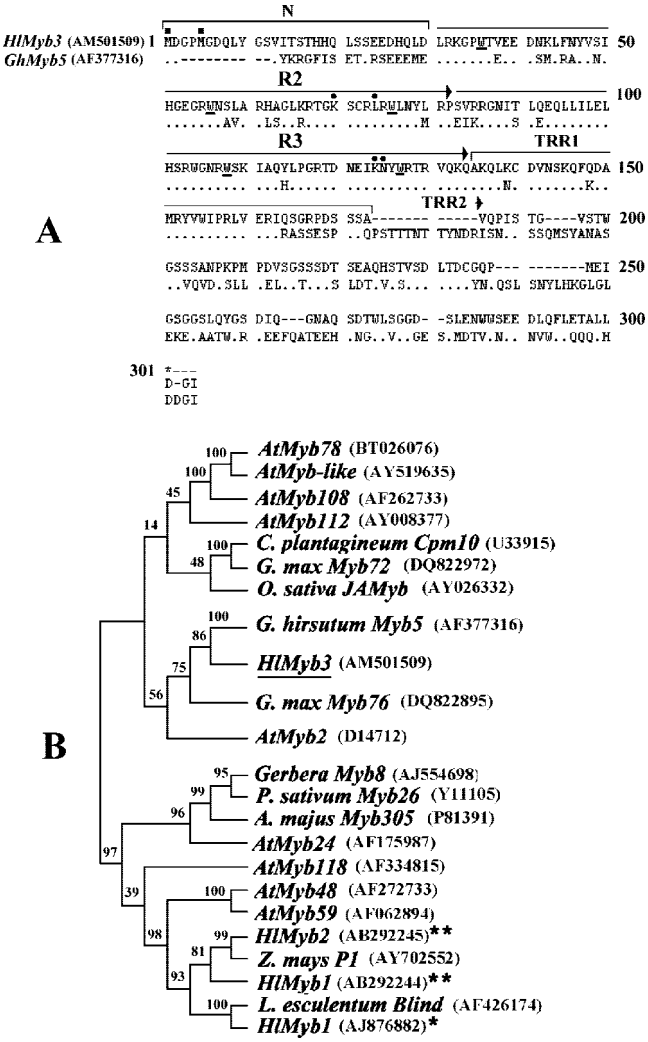

Figure 1. Alignment of deduced amino acid sequences of *HlMyb3* and *GhMyb5* (**A**) and cluster analysis for amino acid sequences of selected plant R2R3 Myb factors (**B**). The structure organization as described for *GhMyb5* (64) is compared with the *HlMyb3* amino acid sequence on panel **A**. R2 and R3 indicate the repeats in the DBD. *N* designates the *N*-terminal segment. TRR1 and TRR2 designate a 40 amino acid basic region and from amino acid position 174 up to the end of the acidic region in the *C*-terminal domain, respectively. Tryptophan residues in *HlMyb3* forming the hydrophobic core are underlined; the filled circles on the top of the sequence indicate conserved DNA base-contacting residues (72); filled squares and arrows designate two starting methionins and the positions of alternative ORFs within the *N*-domain of *HlMyb3*, respectively. Two distinct major clusters on the simplified cladrogram (panel **B**) are designated as I and II. GeneBank AC numbers are given to identify individual sequences. An asterisk designates a *HlMyb* sequence isolated from *Humulus lupulus* in our previous study (*9*); two other hop Myb's available in the GeneBank are designated by double asterisks; *HlMyb3* analyzed in this work is underlined. Fine amino acid sequence alignments and a "neighbor joining" analysis were performed using Dnasis MAX. Values of the confidence of individual branches are shown.

4.23 and the whole protein pI would be 6.43. The predicted shorter 265 aa and the longer 269 aa (*l-HlMyb3*) variants would also differ in mean hydrophobicity and hydrophobic moment, with calculated values of 0.13 and 0.15 for *l-HlMyb3* and 0.20 and 0.32 for *s-HlMyb3*, respectively.

Homology comparisons of *HlMyb3* (*l-HlMyb3* variant) were performed with selected *Myb* factors isolated from the hop and from other plants listed in the NCBI Blast 2 (*33*) search results

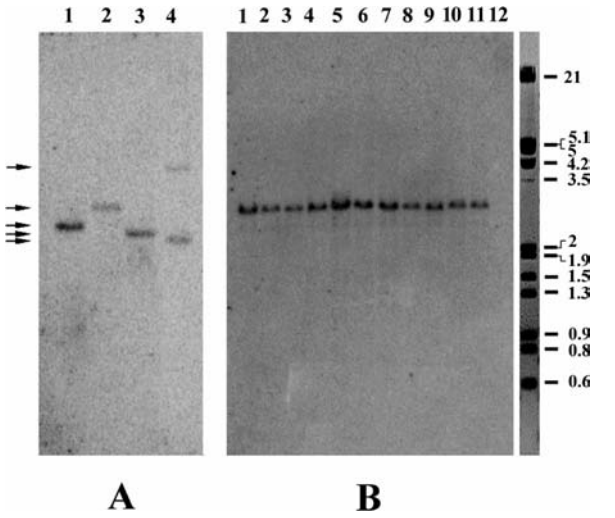

Figure 2. Southern analysis of genomic DNA from the hop with a *HlMyb3*-specific cDNA probe. (**A**) Analysis of Osvald's 72 genomic DNA cleaved with different restriction endonucleases and probed for *HlMyb3*. Lane 1, DNA digested with *Eco*RI; lane 2, *Hin*dIII; lane 3, *Dra*I; lane 4, *Xba*I. (**B**) DNA from 11 hop cultivars and *Humulus japonicus* was cleaved with *Hin*dIII and probed for *HlMyb3*. Lane 1, hop cultivar target; lane 2, hop cv. Eroica; lane 3, hop cv. Galena; lane 4, hop cv. Southern Brewer; lane 5, hop cv. Taurus; lane 6, hop cv. Yeoman; lane 7, hop cv. Cascade; lane 8, hop cv. Brewers Gold; lane 9, hop cv. Osvald's 72; lane 10, hop cv. Agnus; lane 11, hop cv. Columbus; lane 12, *Humulus japonicus*. The DNA marker is aligned on the right side of the autoradiogram.

with significant probability (*E* value in the range from 1e-73 to 9e-33) as provided by the SIB BLAST network service (**Figure 1B**). These comparisons show that *HlMyb3* forms an independent cluster together with *GhMyb5*, while other hop Myb's identified so far show better similarity to P-Myb from *Zea mays* and the Blind TF from tomato. The homology of *HlMyb3* with the previously characterized *HlMyb1* having AC:AJ876882 (*9*) was 54%, suggesting low similarity. Even within the highly conserved DBD, this homology is rather low and reaches only 66% (50% of amino acid identity), indicating functional dissimilarity of these two proteins. *HlMyb3* clustered with ABA-inducible *A. thaliana AtMyb2* (*11*), and some degree of similarity was shared with the cluster of *AtMyb*'s numbered 78, 108, and 112, and classified by Stracke et al. (*31*).

An analysis of hop genomic DNA for the variability of *HlMyb3* sequences was performed with the aim of estimating the number of genes related to *HlMyb3* and the variability of *HlMyb3*-related sequences in selected hop genotypes (**Figure 2**). DNA samples from the genotype of Osvald's 72 that were cleaved with *Eco*RI, *Hin*dIII, *Dra*I, and *Xba*I and probed for the *HlMyb3* gene (**Figure 2A**) showed rather simple patterns on genomic blots. Single fragments were observed for *Eco*RI, *Hin*dIII, and *Dra*I, having 2.4, 2.9, and 2.3 kbp, respectively. Two fragments having 2.2 and 4.0 kbp were observed after *Xba*I digestion, suggesting either the cleavage of *HlMyb3* within some intron(s) or detection of at least two possibly allelic forms of *HlMyb3* genes. An almost invariable *Hin*dIII genomic pattern has been observed for various *H. lupulus* cultivars, lanes 1–11 (**Figure 2B**), while no hybridization signal was observed in lane 12, where *Hin*dIII-digested DNA from *H. japonicus* was applied, suggesting that the *HlMyb3* homolog is either absent in *H. japonicus* or is significantly divergent from the *H. lupulus* sequence.

Analysis of Expression of the Transcription Factor *HlMyb3* in Hop. Although the role of *HlMyb3* cannot be

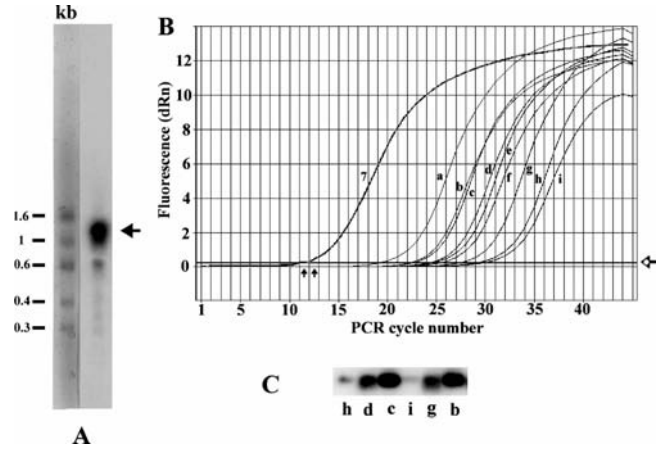

Figure 3. Northern blot, real-time PCR and RT–PCR analyses of *HlMyb3* in the hop. (**A**) Northern blot analysis of RNA isolated from cones of the hop cultivar Osvald's 72. (**B**) Results of real-time PCR using samples from various tissues using either hop oligo dT or 7SLRNA-specific primers as described in the Materials and Methods. (**C**) Molecular hybridization of the 201-bp RT–PCR reaction product to the [α-^{32}P] dCTP-labelled *HlMyb3* probe. The accumulation curves and hybridization products on panels **B** and **C** corresponded to the following tissues: a, leaf tissue of *Arabidopsis thaliana* transformed with 35S-driven *s-HlMyb3* as a standard for strong *Hl*Myb3 expression; b, maturating hop cones, late stage; c, colored petiole epidermis; d, leaves of small soil-grown plants (0.5 m); e, young stems of fully expanded maturating plants (4–5 m); f, leaves from hop plants grown in vitro; g, young maturating cones; h, fully expanded leaves from maturating plants (4–5 m); i, flowers from hop plants (4–5 m). A mean 7SL RNA curve is shown (nr. 7). The arrows on panel **A** show that the major band corresponds to approximately 1.3 kb mRNA of *HlMyb3* and that the RNA molecular weight marker III (Boehringer Mannheim) was applied as a standard (kb). The filled arrows on panel **B** indicate the variability of 7SL RNA cycling; the hollow arrow shows the position of the threshold level.

deduced from similarity with known *A. thaliana* TFs, its expression pattern could contribute to gain some insight into its function. Using a Northern blot analysis of RNA from maturating hop cones using *HlMyb3* cDNA as a probe, a predominant band having approximately 1.3 kb was detected (**Figure 3A**). A real-time PCR procedure was developed for the quantitative analysis of the *HlMyb3* expression in various hop tissues (**Figure 3B**). For real-time cDNA amplification, a 201-bp fragment was selected in the unique *C*-terminal domain of *HlMyb3* to avoid any homology with DBD conserved in various Myb factors (see Materials and Methods). While the 7SL RNA marker showed no significant variability on real-time PCR (**Figure 3B**), suggesting that equal amounts of RNA were applied in individual samples, levels of *HlMyb3* mRNA differed significantly in various tissues. The highest levels in the hop were detected at the late stage of maturating hop cones (curve b) and in the colored epidermis of petioles (curve c). These two samples exceeded the threshold level at 22 cycles. The lowest levels were observed in flowers of maturating hop plants (4–6 m of height; curve i) and in fully expanded leaves of the plants (curve h). It was found by exact comparisons using diluted cloned cDNA as a template that the level in maturating cones was 111 times higher than that in flowers, but 7 times lower than that in the transgenic leaf tissue of *A. thaliana*, where *HlMyb3* expression was driven from the 35S CaMV promoter (**Figure 3B**, curve a). Intermediate levels were detected in young leaves of in vitro hop plants or in stems of young plants. Quantitative changes in the levels of a 201-bp product were observed also after amplification by one-step RT–PCR. Ampli-

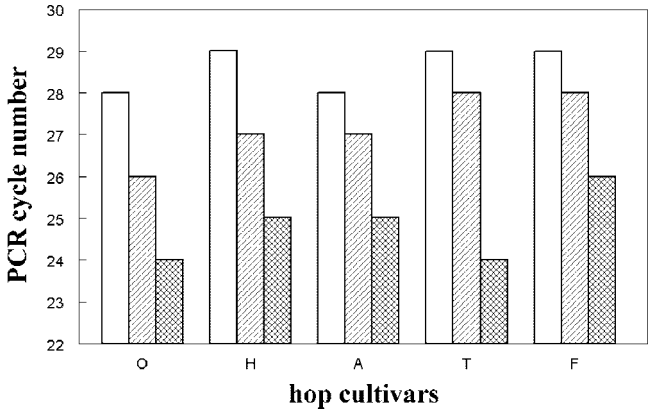

Figure 4. Analysis of *HlMyb3* expression in cones of several hop cultivars by real-time PCR. The dependence on cycle numbers exceeding the threshold level is shown for samples isolated from maturing cones at an early stage (white boxes), an intermediate stage (singly shaded boxes), and a later stage (doubly shaded boxes). Samples were collected from hop cultivars Osvald's clone 72 (O), Hallertau (H), Agnus (A), Taurus (T), and Fuggles (F).

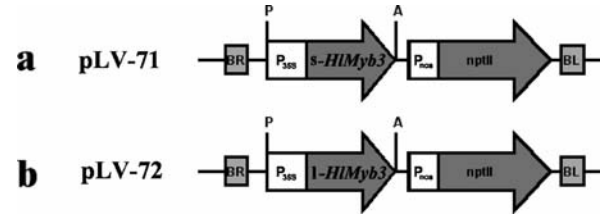

Figure 5. Schematic drawing of expression cassettes within the T-DNA parts of the plant vectors used for transformation. The schemes are not according to scale. (**a**) Vector pLV-71 containing the shorter ORF version of *HlMyb3* (*s-HlMyb3*). (**b**) pLV-72 contains the longer ORF version of *HlMyb3* (*l-HlMyb3*). The *HlMyb3* sequences are driven by the 35S CaMV promoter (P_{35}). Coding sequences are in dark gray, promoters are in white, and T-DNA border sequences are in light gray. NptII designates the neomycin phosphotransferase gene for resistance to kanamycin. This gene is driven by the nopalinsynthase promoter (P_{nos}). BR and BL are the right and left T-DNA borders, respectively. The letters A and P indicate the positions of *Asc*I and *Pac*I restriction sites, respectively. These restriction sites were used for the integration of cassettes in the plant vector.

fied cDNA hybridized with the *HlMyb3* probe (**Figure 3C**), confirming that the product from various tissues was specific. These results suggest that the expression of *HlMyb3* is strongly regulated in developing hops, particularly during the development of hop inflorescences. An increasing accumulation of *HlMyb3* mRNA during hop cone maturation was detected by the real-time analysis also in other hop genotypes, as evaluated from cycle numbers exceeding the threshold level and corresponding to initial product accumulation during thermal cycling (**Figure 4**).

Expression and Biological Effects of *HlMyb3* in Heterologous Plant Transformants. In order to assay the potential function of *HlMyb3*, we did not use direct laborious and time-consuming transformation of the hop (*24*) but instead applied a much more efficient *A. tumefaciens* mediated transformation of *A. thaliana*, *N. benthamiana*, and *P. hybrida* with plant expression vectors containing either *l-HlMyb3* or *s-HlMyb3* ORFs. These vectors were constructed on the basis of ligation of the cDNA expression cassette driven by the 35S CaMV promoter into the previously described vector pLV-62 (*7*). The resulting expression vectors pLV-71 and pLV-72 containing *s-HlMyb3* and *l-HlMyb3* sequences, respectively (**Figure 5**), were introduced into *A. tumefaciens* strains (see Materials and Methods). In the following, we refer to *s-HlMyb3* and *l-HlMyb3* transformation instead of plant vectors for simplicity.

After transformation and selfing, 30 T_2 *s-HlMyb3* and 26 T_2 *l-HlMyb3 A. thaliana* lines resistant to kanamycin were obtained. The presence of the transgene was primarily confirmed by PCR using primers for nptII (not shown), by Southern blots (**Figure 6A**) and by Northern blots for *HlMyb3* transgene expression (**Figure 6B**). The phenotypes of transgenic plants differed from the wild-type Columbia control. In the *l-HlMyb3* lines, a significant retardation in seed germination and initial growth was evident. The *l-HlMyb3* transgenic plants were smaller and rather pale. Adult *l-HlMyb3* plants developed similarly to the wild type, although an obvious delay in the starting of the flowering period was observed (15–20 days). As opposed to the *l-HlMyb3* transgenic plants, *s-HlMyb3* lines exhibited a more rapid start of growth, and adult plants showed a unique branching phenotype with many long lateral stems formed at an angle near 90° (**Figure 7A**). The fertility was not significantly affected by the presence of the *HlMyb3* transgene in both versions, as this was only related to the number and the length of primary and secondary stems.

For more exact comparisons of so-called antagonistic physiological effects of *HlMyb3* ORF variants on initial growth rate, we prepared stable homozygous lines to eliminate transgene segregation. Those T_2 lines were selected that showed a 3:1 ratio between kanamycin-resistant and kanamycin-sensitive plants. After selfings, two homozygous nonsegregating T_3 or T_4 lines of each construct expressing similar quantities of *s-HlMyb3* and *l-HlMyb3* transgenes (**Figure 6B**) were compared for germination and growth capability with a nontransformed control under identical conditions on an MS medium without antibiotics (**Figure 8**). It was clear from these analyses that *s-HlMyb3* seeds germinated even earlier than Columbia wild-type ones and exhibited very vigorous seedlings. On the contrary, the first couple of true leaves appeared nearly 1 week later in *l-HlMyb3* transgenotes in comparison to the wild-type control plants. Also, lateral roots appeared very early (5–7 days after the onset of germination) and developed much more intensively in *s-HlMyb3* transgenotes than in the control, while significant retardation compared to the control was observed for *l-HlMyb3* transgenotes (**Figure 8**, compare samples in panel **C**). We used image analysis (see Materials and Methods) to measure the lengths of roots and leaf areas in in vitro seedlings (**Figure 8**). While 3 days postgermination values of 3.5 ± 1.00, 6.4 ± 0.36, and 1.4 ± 0.13 mm were measured for the control, *s-HlMyb3* and *l-HlMyb3* seedlings reached root lengths of 19.7 ± 1.94, 23.8 ± 3.26, and 13.3 ± 0.77 mm. These data document that the major differences occur during the beginning of germination. At 11 days postgermination, the total leaf areas were measured. While this parameter was 7.7 ± 1.94 mm^2 for the control, 11.8 ± 1.97 mm^2 was measured for *s-HlMyb3* lines and 3.3 ± 0.96 mm^2 for *l-HlMyb3*. These experiments performed on *A. thaliana* plants suggest that there are diverse or so-called antagonistic physiological effects of *s-HlMyb3* versus *l-HlMyb3* transgenes. In addition, our results showed that *HlMyb3* has the potential to interfere in *A. thaliana* morphogenesis.

A total of 23 trangenotes of *s-HlMyb3* and 28 of *l-HlMyb3* of *N. benthamiana* resistant to kanamycin and expressing the transgenes as shown in **Figure 6C** were also obtained. In comparison to the effects observed for *A. thaliana*, *N. benthamiana* plants exhibited more distinct changes in growth and

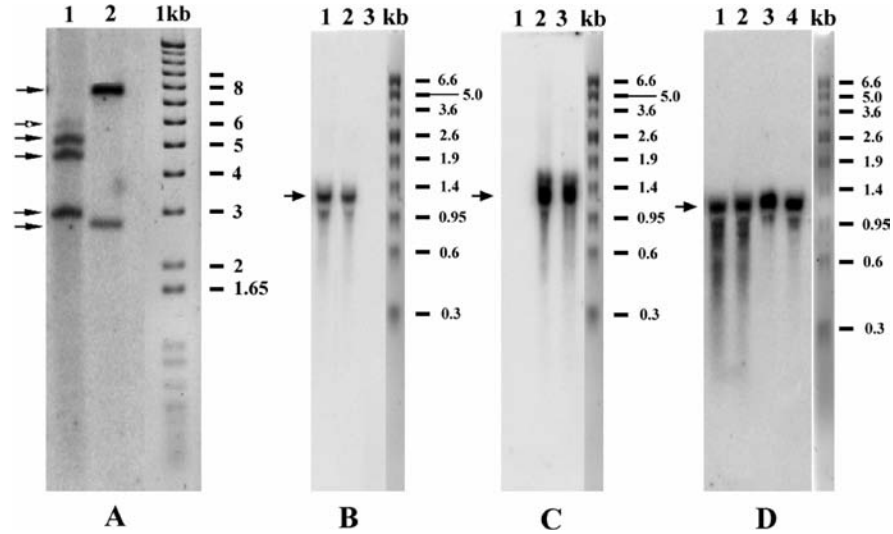

Figure 6. Example of Northern blot analysis of plants transformed with HlMyb3 constructs. (**A**) Example of genomic blots of *Eco*RI-cleaved DNA from *A. thaliana* transgenotes. 1, *l-HlMyb3* (line 1812/11f); 2, *s-HlMyb3* (line 1811/8a). DNA marker is aligned on the right side of the autoradiogram. (**B**–**D**) Examples of Northern blot analyses. Total RNA isolated from *Arabidopsis thaliana* seedlings (**B**), *Nicotiana benthamiana* (**C**), and *Petunia hybrida* (**D**) transgenotes. (**B**) 1, *s-HlMyb3* (line 1811/8c); 2, *l-HlMyb3* (line 1812/11f); 3, control plant ecotype Columbia. (**C**) 1, untransformed *N. benthamiana*; 2, *l-HlMyb3* (line 1812/8); 3, *s-HlMyb3* (line 1811/4). (**D**) 1, *l-HlMyb3* (line 1774/2), young leaves; 2, *l-HlMyb3* (line 1774/2), old leaves; 3, *s-HlMyb3* (line 1773/1), young leaves; 4, *s-HlMyb3* (line 1773/1), old leaves. No signals were detectable in samples from untransformed *P. hybrida* plants. A probe derived from the cDNA of *HlMyb3* was used for hybridization (see Materials and Methods). The positions of the main specific bands having about 1.2–1.3 kb are indicated by arrows; the positions of Promega RNA markers are indicated on the right side.

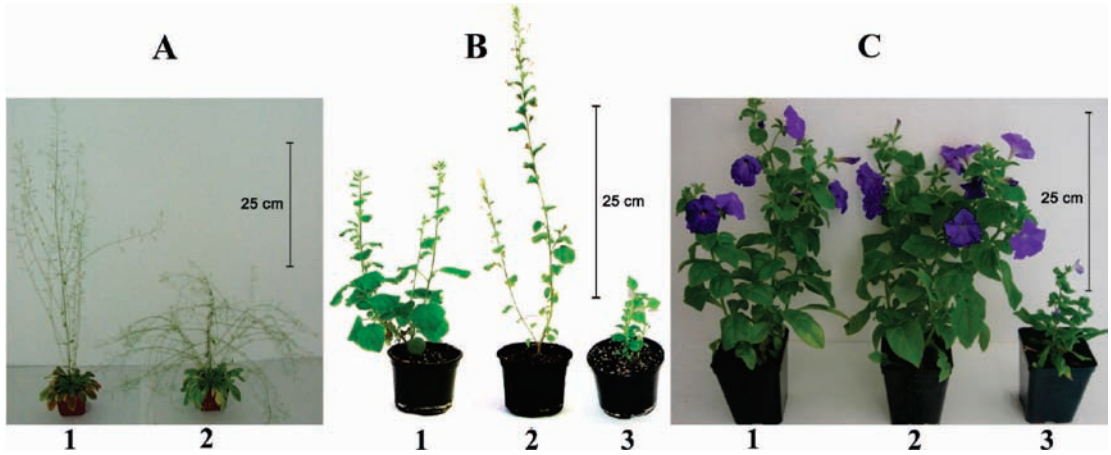

Figure 7. Examples of phenotypes of *Arabidopsis thaliana* (**A**), *Nicotiana benthamiana* (**B**), and *Petunia hybrida* (**C**) transformed with ORF variants of *HlMyb3*. In panel **A**, the *A. thaliana* control, i.e., the ecotype Columbia (1), and the transgenic plant line T_3 1811/8e bearing the *s-HlMyb3* transgene (2) and having a changed branching phenotype are shown. Transgenic lines bearing the *l-HlMyb3* transgene did not differ in shape from that of the controls. In panel **B**, the *N. benthamiana* control (1) is compared with characteristic transgenotes bearing *s-HlMyb3* line 1811/4 (2) and *l-HlMyb3* line 1812/8 (3). In panel **C**, petunia transgenotes are compared with the nontransformed control (1). Sample 2 represents line *s-HlMyb3* No 1773/1 and sample 3 line *l-HlMyb3* No 1774/2.

development. All transgenic plants overexpressing the *HlMyb3* ORF variants had significantly reduced fertility, and in the case of *l-HlMyb3*, the transgenic plants were completely sterile. The sterility was probably related to the dwarfism observed for *l-HlMyb3* plants (compare *N. benthamiana* transgenotes in **Figure 7B**). Also, apical dominancy of the primary stem was inhibited. The *s-HlMyb3* plants showed a higher main stem with few long branches at the base. The leaves were small and narrow; the nodes were ordered more thickly on the stem in comparison to the wild-type plant (**Figure 7B**). The flowers for both ORF variants overexpressing the *HlMyb3* gene were smaller with a very close cylinder of the calyx and trumpet-shaped corolla tubes. Due to sterility of most of the *l-HlMyb3* overexpressing *N. benthamiana* plants, we were not able to get T_2 or T_3 generations, and the plants had to be propagated vegetatively in aseptical conditions through regenerations of the leaf or apical stem explants.

A total of 12 and 15 plant regenerants of *P. hybrida* transformed with *s-HlMyb3* and *l-HlMyb3*, respectively, and rooting on kanamycin were selected. *P. hybrida* transgenotes expressing *s-HlMyb3* and *l-HlMyb3* variants (**Figure 6D**) also exhibited diverse phenotypic effects. While for plants transformed with *s-HlMyb3* partial sterility, but rather branchy phenotypes similar to controls (**Figure 7C**, compare samples 1 and 2) was characteristic, some strong developmental distortions like a strong dwarfism, inhibited apical dominancy, leaf curling, and complete sterility were reproducibly observed for *l-HlMyb3* transgenotes (**Figure 7C**, sample 3). The results obtained on these two solanaceous species confirmed an involvement of *HlMyb3* transgenes in morphogenetic changes.

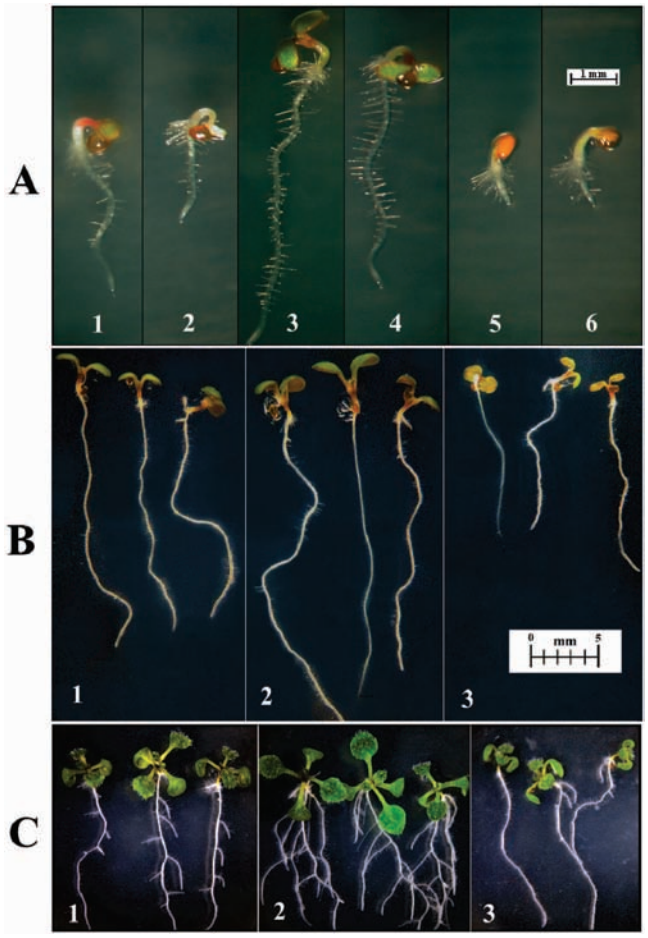

Figure 8. Example of initial germination and growth of *HlMyb3* transgenic seedlings of *Arabidopsis thaliana* under in vitro conditions. (**A**) Germination three days postsow (dps): 1 and 2, control seedlings of the ecotype Columbia; 3 and 4, *s-HlMyb3* transgenotes; 5 and 6, *l-HlMyb3* transgenes. (**B**) The growth of seedlings 6 dps: 1, control; 2, *s-HlMyb3*; 3, *l-HlMyb3*. (**C**) Branching 11 dps; 1, control; 2, *s-HlMyb3*; 3, *l-HlMyb3*. *s-HlMyb3* and *l-HlMyb3* bear T_2 lines 1811/8e and 1812/11f.

Changes in the Composition of Secondary Metabolites in Plants Transformed with *HlMyb3* ORFs. According to our results, *HlMyb3* is strongly regulated in hop, and the highest levels were detected in the colored petiole epidermis and in hop cones at a late stage of maturation (**Figure 3**). During this stage, an intensive synthesis of secondary metabolites occurs in the lupulin glands (*1*), and anthocyanin pigmentation appears in the epidermis of the hop cone bracts. Therefore, we addressed the question as to whether there is some potential of *HlMyb3* to influence the composition of secondary metabolites, more specifically phenolic acids and flavonol glycosides, in heterologous transgenotes.

Extracts from *A. thaliana*, *N. benthamiana*, and *P. hybrida* leaf samples were prepared (see Materials and Methods), and HPLC analyses were performed. Chromatograms of all plant samples at 320 and 350 nm were extracted from the 3D data, and peaks were characterized on the basis of their retention times and UV spectra and mass spectral data for *A. thaliana* samples (**Table 1**). Results in **Table 1** are indicative compositional changes in transgenotes as compared to the controls. Differences appear not only between nontransformed plants and *A. thaliana* transgenic lines (compare, e.g., peaks representing phenolic acids with retention times of 11.0, 12.7, 13.8, and 20.0 min and lower levels of flavonol glycosides in comparison to the control) but also between *s-HlMyb3* and *l-HlMyb3 A. thaliana* transgenotes (compare peaks representing phenolic acids with retention times of 11.0 and 20.0 min). In general, a decrease is noted in the presence of secondary metabolites from *A. thaliana* transgenotes in comparison to nontransformed controls. However, changes are rather moderate in comparison to the accumulation of metabolites that seems to be characteristic for the *A. thaliana* line overexpressing the inductor of anthocyanin biosynthesis *Pap-1* (*34*) (**Table 1**, column 4). In *N. benthamiana* and *P. hybrida* transgenotes, some phenolic acids and flavonol glycosides accumulated to much higher levels in comparison to the controls (compare, e.g., *N. benthamiana* peaks representing phenolic acids with retention times of 27.4 min and the fraction of flavonol glycosides and *P. hybrida* peaks representing phenolic acids with retention times of 13.0, 14.1, and 29.4 min). Except for the phenolic acids fraction of *N. benthamiana*, notably the peak with a retention time of 14.1 min, and of *P. hybrida*, notably the peak with a retention time of 21.1 min, that

Table 1. Normalized Peak Areas for Secondary Metabolites in Methanol/Water Extracts from *Arabidopsis thaliana*, *Nicotiana benthamiana*, and *Petunia hybrida* Transformants and Control Plants[a]

R_t (min)	λ_{max} (nm)	1[b]	2[b]	3[b]	4[b]
Major Peaks at 320 nm (Phenolic Acids) in *Arabidopsis thaliana*					
11.0	295	1	0.91	1.73	1.37
12.7	329–332	1	0.89	1.26	9.98
13.8	277–322	1	0.58	0.62	3.31
20.0	327	1	1.43	2.92	7.76
21.1	322	n.d.	n.d.	0.23	1.00
Major Peaks at 350 nm (Flavonol Glycosides) in *Arabidopsis thaliana*					
12.1[c]	256–353	n.d.	n.d.	n.d.	1.00
13.4[c]	266–345	1	0.65	0.46	1.04
15.9	256–351	n.d.	n.d.	n.d.	1.00
19.0	266–342	1	0.71	0.37	1.02
19.5	349	1	0.57	0.64	1.14
21.9[c]	263–341	1	0.78	0.44	1.02

R_t (min)	λ_{max} (nm)	1[b]	2[b]	3[b]
Major Peaks at 320 nm (Phenolic Acids) in *Nicotiana benthamiana*				
11.0	327	1	2.06	1.10
11.6	327	1	2.64	1.06
14.1	321	1	1.09	5.14
27.4	318	1	30.31	16.67
Major Peaks at 350 nm (Flavonol Glycosides) in *Nicotiana benthamiana*				
12.6	265–344	1	11.08	3.10

R_t (min)	λ_{max} (nm)	1[b]	2[b]	3[b]
Major Peaks at 320 nm (Phenolic Acids) in *Petunia hybrida*				
13.0	331	1	6.58	3.60
13.6	323	1	2.44	1.14
14.1	327	1	4.95	1.51
14.5	329	1	0.68	0.99
15.5	334	1	1.33	0.99
16.1	331	1	3.04	1.29
20.4	328	1	2.97	2.00
21.1	266–334	1	1.18	6.50
21.6	323	1	2.11	1.33
29.4	330	1	13.23	7.95

[a] n.d.: not detected. The results represent mean values. The coefficient of variation was <10% for all samples. [b] *Arabidopsis thaliana* lines: 1, wild type cv. Columbia; 2, s-HlMyb3(No1811/); 3, l-HlMyb3(No1812/); 4, AP1 (NASC ID:N3884). *Nicotiana benthamiana* lines: 1, wild type; 2, s-HlMyb3(No1811/); 3, l-HlMyb3(No1812/). *Petunia hybrida* lines: 1, wild type; 2, s-HlMyb3(No1773/1); 3, l-HlMyb3 (No1774/2). [c] On the basis of HPLC-MS data and comparisons with the paper of Tohde et al. (*38*), compounds with retention times of 12.1 min (ESI-MS (*m/z*): 757 $[M]^+$), 13.4 min (ESI-MS (*m/z*): 741 $[M]^+$), and 21.9 min (ESI-MS (*m/z*): 579 $[M]^+$) were tentatively identified as quercetin 3-*O*-[6″-*O*-(rhamnosyl-)glucoside] 7-*O*-rhamnoside, kaempferol 3-*O*-[6″-*O*-(rhamnosyl)glucoside] 7-*O*-rhamnoside, and kaempferol 3-*O*-rhamnoside 7-*O*-rhamnoside, respectively.

were detected in higher levels in the extracts from *l-HlMyb3* than in those from *s-HlMyb3* transgenotes, all other significant differences indicate increased levels of secondary metabolites in *s-HlMyb3* transgenotes in comparison to *l-HlMyb3* transgenic lines.

DISCUSSION

Developmental Regulation of *HlMyb3* Expression in Hop and Similarity of *HlMyb3* to *GhMyb5* and to Other TFs. The present study concerned cloning and partly characterizing *HlMyb3*, a putative transcription factor of the hop, using a previously constructed tissue-specific cDNA library (*7*, *9*). Our genomic analyses suggest that *HlMyb3* is a rather unique gene, which can be detected in various hop cultivars, but a homologous sequence was absent in the species *H. japonicus*. As derived from BLAST comparisons, *HlMyb3* shows the highest homology to *GhMyb5* from cotton, which has been characterized by Loguercio et al. (*32*) and Cedroni et al. (*35*) as a unique sequence that diverges from other *Myb* TF sequences isolated from cotton fiber tissues. Besides structural similarities of *HlMyb3* and *GhMyb5* regarding amino acid levels, particularly within the DBD amounting to 91%, some similarity in the expression of these two genes is noted. Although the function of *GhMyb5* is not known, this TF-encoding mRNA is abundant in bracts, but much lower levels are observed in leaves and in floral organs like ovules or pollen, suggesting strong developmental regulation (*32*). *HlMyb3* mRNA showed the lowest concentrations in hop flowers and high concentrations in maturing hop cones, where lupulin glands develop on the inner side of the bracts. High concentrations of *HlMyb3* mRNA were detected also in the colored epidermis of petioles, indicating potential relevance of this TF in tissues where flavonoid biosynthesis occurs. *HlMyb3* is quite unrelated to the first Myb TF isolated from hop designated *HlMyb1*, which seems related to P-Mybs (*23*) and to the Blind factor from tomato (*15*), and occurs in a quite different cluster on the genealogy trees. In addition to the high degree of divergence, these two TFs differ also in patterns of expression. While *HlMyb1* was most abundant in hop female and male flowers and absent in cones as revealed by Northern blots (*9*), *HlMyb3* showed an opposite pattern of expression in hop inflorescences, suggesting an unrelated function(s) of these two TFs.

Structure of *HlMyb3* and Antagonistic Action of *HlMyb3* ORF Variants. It was described that the *GhMyb5* sequence contains alternative ORFs in the 5′-leader sequence, and it was speculated that these ORFs may serve to regulate the biosynthesis of this particular *GhMyb* protein at the translational level (*32*). We found two initiating ATG codons in the 5′-terminal part of *HlMyb3* cDNA. Corresponding ORFs code for the longer or shorter *N*-terminal domain of *HlMYB3*, which is unique and quite unrelated to *GhMyb5*. Two alternative expression vectors were constructed to overexpress either shorter *s-HlMyb* or longer *l-HlMyb* variants in heterologous transgenotes. Our analyses show that both ORF variants are active transgenes that interfere in plant morphogenesis, growth, and composition of the plant metabolome. Surprisingly, the activity of *s-HlMyb* versus *l-HlMyb* seems to be so-called independently antagonistic on transgene mRNA levels in individual transgenotes. While, in general, *s-HlMyb3* is stimulatory, *l-HlMyb3* caused a delay of growth and some developmental distortions like dwarfing and sterility in solanaceous species. Our observations suggest that, in fact, the *N*-terminal domain in *HlMyb3* is responsible for differential interaction of *HlMyb3* variants with some factors and cellular components. It is not known whether or not these factors interact with the protein *N*-terminus directly or whether this interaction is rather mediated by some structural changes in other parts of the corresponding *s-HlMyb3* and *l-HlMyb3* proteins. In particular, the highly variable *C* part of R2R3 Mybs containing the transactivation domain (*32*) is considered to be responsible for differential protein–protein interactions (*11*, *31*). According to our predictions, *s-HlMyb3* and *l-HlMyb3* differ in parameters like pI and hydrophobicity, although the difference in predicted protein mass is not dramatic. It does not follow from our experiments whether or not both *HlMyb3* forms showing antagonistic biological activities in heterologous transgenotes exist in the hop. However, there could be some mechanisms such as differential translation that could cause their accumulation.

Diverse Phenotypic Effects of *HlMyb3* in Heterologous Transgenotes. There are diverse biological effects caused by *HlMyb3* variants in various transformed plant species. For instance, *s-HlMyb3* causes in *A. thaliana* a quite unique phenotype with many long lateral branches formed at an angle near 90°. A similar phenotype was not observed for either *N. benthamiana* or *P. hybrida s-HlMyb3* transgenotes, although these plants showed rather branching phenotypes. *HlMyb3* variants caused some degree of sterility in both solanaceous species, while there was no significant effect on the sterility of *A. thaliana*. While *HlMyb3* transgene variants led to lower levels of pigment accumulation in *A. thaliana* in comparison to the controls, a dramatic accumulation of some flavonol glycosides and phenolic acids was noted in both transformed solanaceous species. These observations can be explained by a different character of combinatorial TFs (*20*) that are present in individual species or appear under different physiological conditions and interact with *HlMyb3* transgene variants. Such examples are known, for instance, from regulations of the phenylpropanoid pathway (*10*). These combinatorial TFs could be Myc, bHLH, or bZIP regulatory factors (e.g., refs (*12*), (*19*), and (*36*)). By combinatorial interactions with other TFs, a pleiotropic effect and an involvement of *HlMyb3* transgene variants into various processes like morphogenesis and metabolome modifications can be explained. These effects on heterologous transgenotes suggest that the *HlMyb3* gene encoding a putative myb factor in the hop has the potential to influence hop morphogenesis and possibly hop bine anatomy as an important genetic trait that may codetermine the yield of hop cones, as well as the metabolome composition during lupulin maturation.

ACKNOWLEDGMENT

We thank Dr. Lukáš Vrba from BC v.v.i. IPMB, České Budějovice, Czech Republic, for the preparation of plant expression vectors. We are indebted to Mrs. Helena Matoušková, Ing. Olga Horáková, and Ing. Lidmila Orctová (BC v.v.i. IPMB, České Budějovice, Czech Republic) for their help and technical assistance.

LITERATURE CITED

(1) De Keukeleire, J.; Ooms, G.; Heyerick, A.; Roldán-Ruiz, I.; Van Bockstaele, E.; De Keukeleire, D. Formation and accumulation of α-acids, β-acids, desmethylxanthohumol and xanthohumol during flowering of hops (*Humulus Lupulus* L.). *J. Agric. Food Chem.* **2003**, *51*, 4436–4441.

(2) Stevens, J. F.; Page, J. E. Xanthohumol and related prenylflavonoids from hops and beer: to your good health. *Phytochemistry* **2004**, *65*, 13171330.

(3) Gerhäuser, C.; Alt, A.; Heiss, E.; Gamal-Eldeen, A.; Klimo, K.; Knauft, J.; Neumann, I.; Scherf, H. R.; Frank, N.; Bartsch, H.; Becker, H. Cancer chemopreventive activity of xanthohumol, a natural product derived from hop. *Mol. Cancer Ther.* **2002**, *1*, 959–969.

(4) Milligan, S. R.; Kalita, J. C.; Heyerick, A.; Rong, H.; De Cooman, L.; De Keukeleire, D. Identification of a potent phytoestrogen in hops (*Humulus lupulus* L.) and beer. *J. Clin. Endocrinol. Metab.* **1999**, *84*, 2249–2252.

(5) Matoušek, J.; Novák, P.; Bříza, J.; Patzak, J.; Niedermeierová, H. Cloning and characterisation of chs-specific DNA and cDNA sequences from hop (*Humulus lupulus* L.). *Plant Sci.* **2002**, *162*, 1007–1018.

(6) Okada, Y.; Ito, K. Cloning and analysis of valerophenone synthase gene expressed specifically in lupulin gland of hop (*Humulus lupulus* L.). *Biosci. Biotechnol. Biochem.* **2001**, *65*, 150–155.

(7) Matoušek, J.; Vrba, L.; Škopek, J.; Orctová, L.; Pešina, K.; Heyerick, A.; Baulcombe, D.; De Keukeleire, D. Sequence analysis of a "true" chalcone synthase (*chs*_H1) oligofamily from hop (*Humulus lupulus* L.) and PAP1 activation of chs_H1 in heterologous systems. *J. Agric. Food Chem.* **2006**, *54*, 7606–7615.

(8) Novák, P.; Krofta, K.; Matoušek, J. Chalcone synthase homologues from *Humulus lupulus*: some enzymatic properties and expression. *Biol. Plant* **2006**, *50*, 48–54.

(9) Matoušek, J.; Vrba, L; Novák, P.; Patzak, J.; De Keukeleire, J.; Škopek, J.; Heyerick, A.; Roldán-Ruiz, I.; De Keukeleire, D. Cloning and molecular analysis of the regulatory factor *Hl*Myb1 in hop (*Humulus lupulus* L.) and the potential of hop to produce bioactive prenylated flavonoids. *J. Agric. Food Chem.* **2005**, *53*, 4793–4798.

(10) Broun, P. Transcription factors as tools for metabolic engineering in plants. *Curr. Opin. Plant Biol.* **2004**, *7*, 202–209.

(11) Kranz, H. D.; Denekamp, M.; Greco, R.; Jin, H.; Leyva, A.; Meissner, R. C.; Petroni, K.; Urzainqui, A.; Bevan, M.; Martin, C.; Smeekens, S.; Tonelli, C.; Paz-Ares, J.; Weisshaar, B. Towards functional characterisation of the members of *the R2R3-MYB* gene family from *Arabidopsis thaliana*. *Plant J.* **1998**, *16*, 263–276.

(12) Ramsay, N. A.; Glover, B. J. MYB–bHLH–WD40 protein complex and the evolution of cellular diversity. *Trends Plant Sci.* **2005**, *10*, 63–70.

(13) Carlsbecker, A.; Helariutta, Y. Phloem and xylem specification: pieces of the puzzle emerge. *Curr. Opin. Plant Biol.* **2005**, *8*, 512–517.

(14) Talbert, P. B.; Adler, H. T.; Parks, D. W.; Comai, L. The *REVOLUTA* gene is necessary for apical meristem development and for limiting cell divisions in the leaves and stems of *Arabidopsis thaliana*. *Development* **1995**, *121*, 2723–2735.

(15) Schmitz, G.; Tillmann, E.; Carriero, F.; Fiore, C.; Cellini, F.; Theres, K. The tomato Blind gene encodes a MYB transcription factor that controls the formation of lateral meristems. *Proc. Natl. Acad. Sci. U.S.A.* **2002**, *99*, 1064–1069.

(16) Schmitz, G.; Theres, K. Shoot and inflorescence branching. *Curr. Opin. Plant Biol.* **2005**, *8*, 506–511.

(17) Kirik, V.; Lee, M. M.; Wester, K.; Herrmann, U.; Zheng, Z.; Oppenheimer, D.; Schiefelbein, J.; Hulskamp, M. Functional diversification of *MYB23* and GL1 genes in trichome morphogenesis and initiation. *Development* **2005**, *132*, 1477–1485.

(18) Gruber, M. Y.; Wang, S.; Ethier, S.; Holowachuk, J.; Bonham-Smith, P. C.; Soroka, J.; Lloyd, A. "HAIRY CANOLA"–Arabidopsis GL3 induces a dense covering of trichomes on *Brassica napus* seedlings. *Plant Mol. Biol.* **2006**, *60*, 679–698.

(19) Yamazaki, M.; Makita, Y.; Springob, K.; Saito, K. Regulatory mechanisms for anthocyanin biosynthesis in chemotypes of *Perilla frutescens* var. crispa. *Biochem. Eng. J.* **2003**, *14*, 191–197.

(20) Singh, K. B. Transcriptional regulation in plants: the importance of combinatorial control. *Plant Physiol.* **1998**, *118*, 1111–1120.

(21) Aharoni, A.; de Vos, C. H. R.; Wein, M.; Sun, Z.; Greco, R.; Kroon, A.; Mol, J. N. M.; O'Connell, A. P. The strawberry *FaMYB1* transcription factor suppresses anthocyanin and flavonol accumulation in transgenic tobacco. *Plant J.* **2001**, *28*, 319–332.

(22) Vannini, C.; Locatelli, F.; Bracale, M.; Magnani, E.; Marsoni, M.; Osnato, M.; Mattana, M.; Baldoni, E.; Coraggio, I. Overexpression of the rice *Osmyb4* gene increases chilling and freezing tolerance of *Arabidopsis thaliana* plants. *Plant J.* **2004**, *37*, 115–127.

(23) Zhang, P.; Chopra, S.; Peterson, T. A segmental gene duplication generated differentially expressed myb-homologous genes in maize. *Plant Cell* **2000**, *12*, 2311–2322.

(24) Horlemann, C.; Schwekendiek, A.; Höhnle, M.; Weber, G. Regeneration and *Agrobacterium*-mediated transformation of hop (*Humulus lupulus* L.). *Plant Cell Rep.* **2003**, *22*, 210–217.

(25) Töpfer, R.; Matzeit, V.; Gronenborn, B.; Schell, J.; Steinbiss, H. H. A set of plant expression vectors for transcriptional and translational fusions. *Nucl. Acids Res.* **1987**, *15*, 5890.

(26) Clough, S. J.; Bent, A. F. Floral dip: a simplified method for Agrobacterium -mediated transformation of *Arabidopsis thaliana*. *Plant J.* **1998**, *16*, 735–743.

(27) Matoušek, J.; Junker, V.; Vrba, L.; Schubert, J.; Patzak, J.; Steger, G. Molecular characterization and genome organization of 7SL RNA genes from hop (*Humulus lupulus* L.). *Gene* **1999**, *239*, 173–183.

(28) Matoušek, J.; Trněná, L.; Svoboda, P.; Oriniaková, P.; Lichtenstein, C. P.The gradual reduction of viroid levels in hop mericlones following heat therapy: A possible role for a nuclease degrading dsRNA. *Biol. Chem. Hoppe–Seyler* **1995**, *376*, 715–721.

(29) Rogers, S. O.; Bendich, A. J. Extraction of total cellular DNA from plants, algae and fungi. In *Plant Molecular Biology*, 2nd ed.; Gelvin, S. B., Schilperoort, R. A., Eds; Kluwer, Dodrecht: The Netherlands, 1994; D1, pp 1–8.

(30) Church, G. M.; Gilbert, W. Genomic Sequencing. *Proc. Natl. Acad. Sci. U.S.A.* **1984**, *81*, 1991–1995.

(31) Stracke, R.; Werber, M.; Weisshaar, B. The *R2R3-MYB* gene family in Arabidopsis thaliana. *Curr. Opin. Plant Biol.* **2001**, *4*, 447–456.

(32) Loguercio, L. L.; Zhang, J. Q.; Wilkins, T. A. Differential regulation of six novel *MYB*-domain genes defines two distinct expression patterns in allotetraploid cotton (*Gossypium hirsutum* L.). *Mol. Gen. Genet.* **1999**, *261*, 660–671.

(33) Altschul, S. F.; Madden, T. L.; Schäffer, A. A.; Zhang, J.; Zhang, Z.; Miller, W.; Lipman, D. J. Gapped BLAST and PSI-BLAST: a new generation of protein database search programs. *Nucleic Acids Res.* **1997**, *25*, 3389–3402.

(34) Borevitz, J. O.; Xia, Y.; Blount, J.; Dixon, R. A.; Lamb, C. Activation tagging identifies a conserved MYB regulator of phenylpropanoid biosynthesis. *Plant Cell* **2000**, *12*, 2383–2394.

(35) Cedroni, M. L.; Cronn, R. C.; Adams, K. L.; Wilkins, T. A.; Wendel, J. F. Evolution and expression of *MYB* genes in diploid and polyploid cotton. *Plant Mol. Biol.* **2003**, *51*, 313–325.

(36) Feldbrügge, M.; Sprenger, M.; Dinkelbach, M.; Yazaki, K.; Harter, K.; Weisshaar, B. Functional analysis of a light-responsive plant bZIP transcriptional regulator. *Plant Cell* **1994**, *6*, 1607–1621.

(37) Martin, C.; Paz-Ares, J. MYB transcription factors in plants. *Trends Genet.* **1997**, *13*, 67–73.

(38) Tohde, T.; Nishiyama, Y.; Hirai, M. Y.; Yano, M.; Nakajima, J.; Awazuhara, M.; Inoue, E.; Takahashi, H.; Goodenowe, D. B.; Kitayama, M.; Noji, M.; Yamazaki, M.; Saito, K. Functional genomics by integrated analysis of metabolome and transcriptome of Arabidopsis plants over-expressing an MYB transcription factor. *Plant J.* **2005**, *42*, 218–235.

Received for review April 20, 2007. Revised manuscript received July 13, 2007. Accepted July 19, 2007. The work was supported by Grants GAČR 521/03/0072 and AV0Z50510513, as well as by Grants MŠMT 1-2006-01 and 01S00906 (Special Research Fund of the Ghent University, Ghent, Belgium) within a bilateral collaboration research project between the Czech Republic and Flanders.

JF071153+